

# High output efficiency (340 lm/W) in a one wavelength microcavity OLED

Mitchell C. Nelson

(Dated: 9 March 2015)

An OLED architecture is described in which a thin emitter layer is located at the anti-node of a resonant microcavity. In two realizations, the mode space is constrained by either multi-layer mirrors or by an emitter with transition dipole moments oriented normal to the vertical mode of the device. The multi-layer mirror device achieves 315 lm/W and the oriented emitter device achieves 340 lm/W. Output is observed to be linear in current and efficiency increases with power. This is in agreement with a proposed theoretical model for a microcavity device with emitter located at an anti-node where spontaneous emission is suppressed.

## I. INTRODUCTION

Efficiency for producing light has significant consequences for society. Energy consumption for global lighting produces 2 billion tons of CO<sub>2</sub> each year, 20% of which is produced by 1.6 billion people burning kerosene and paraffin<sup>1</sup> accounting for 7% of all energy related black carbon climate forcing.<sup>2</sup> Improving lighting efficiency is widely recognized as an important measure to help mitigate sources of climate change.<sup>3</sup> OLEDs may contribute to this to the extent that they meet or exceed the efficiency of other lighting devices and improve the environmental footprint for manufacturing and using lighting devices. Efficiency has been a focus of OLED research since the first devices were announced<sup>4567</sup> for these reasons and as a proxy for understanding certain aspects of OLED device physics.

External quantum efficiency, defined as photons extracted per charge injected, has been described as a product of four processes,<sup>8</sup>

$$\eta_{EQE} = \gamma \eta_{S/T} q_{eff} \eta_{out} \quad (1)$$

where  $\gamma$  is the charge carrier balance factor (the fraction of the charge carrier currents that forms electron-hole pairs),  $\eta_{S/T}$  is the singlet-triplet factor (the fraction of radiative excited state species formed from charge carrier recombination),  $q_{eff}$  is the quantum efficiency of the radiative species (the fraction that decay radiatively), and  $\eta_{out}$  is the out-coupling factor (the fraction of photons that exit the device through the intended exit face). It is widely held that out-coupling is now the remaining challenge to external efficiency, and much work has focused on this in recent years<sup>9</sup>

though important advances have been obtained in devices that address out-coupling alongside other ohmic and energetic loss mechanisms.<sup>10</sup>

Efficiency droop, also called roll-off, where efficiency decreases with increasing power output, is still a common feature of OLEDs. Droop can be caused by triplet-triplet annihilation and triplet-polaron quenching as the number density of excited state species increases.<sup>1112</sup> This is in addition to ohmic losses and decreased carrier balance for devices that operate over a large voltage range.

The device reported here uses a microcavity to create a low threshold for output from stimulated emission coupled to a vertical cavity mode with spontaneous emission into the mode forbidden. The vertical mode directly addresses out-coupling and other loss mechanisms appear as a constant offset in a linear relationship between current and light. The resulting device exhibits current driven behavior with bias approaching an asymptote within about 0.2V of turn-on. Thus external and internal efficiencies are addressed by shifting the process to stimulated emission resulting in a high efficiency device with no droop.

In the following, we describe microcavity enhancement and suppression of spontaneous emission, and then consider rate equations for a microcavity OLED and derive efficiency for operation in both limiting cases, a device dominated by stimulated emission and a device dominated by spontaneous emission with varying levels of cavity enhancement. We then report first results for two stimulated emission devices.

## II. OPTICAL MICROCAVITIES

For a microcavity of optical length  $L(\lambda)$ , formed between parallel planar mirrors of reflectivity  $R_1$  and  $R_2$ , with an emitter (spontaneous emission) located at optical distance  $x(\lambda)$  from the  $R_1$  mirror, the normalized intensity of light exiting the  $R_2$  and is given by

$$\frac{|E_{cav}(\lambda)|^2}{|E_{free}(\lambda)|^2} = \frac{(1 - R_2) \left[ 1 + R_1 + 2\sqrt{R_1} \cos(4\pi \frac{x(\lambda)}{\lambda}) \right]}{1 + R_1 R_2 - 2\sqrt{R_1 R_2} \cos(4\pi \frac{L(\lambda)}{\lambda})} \quad (2)$$

where the optical lengths are calculated as a sum over index of refraction times the mechanical length for each intervening layer, plus the penetration depth for each reflector.<sup>1314</sup>

The significance of this for layered electroluminescent devices is illustrated in the following figure, where the normalized output from spontaneous emission is calculated for a one wavelength cavity, with reflectivities 1.0 and 0.8, and free space line-width 0.10. As is evident in FIG. 1, spontaneous emission is completely suppressed for a thin emitter located at the anti-nodes,  $x(\lambda) = \lambda/4$  and  $x(\lambda) = 3\lambda/4$ , and strongly enhanced in the region of the node at  $x(\lambda) = \lambda/2$ . This is

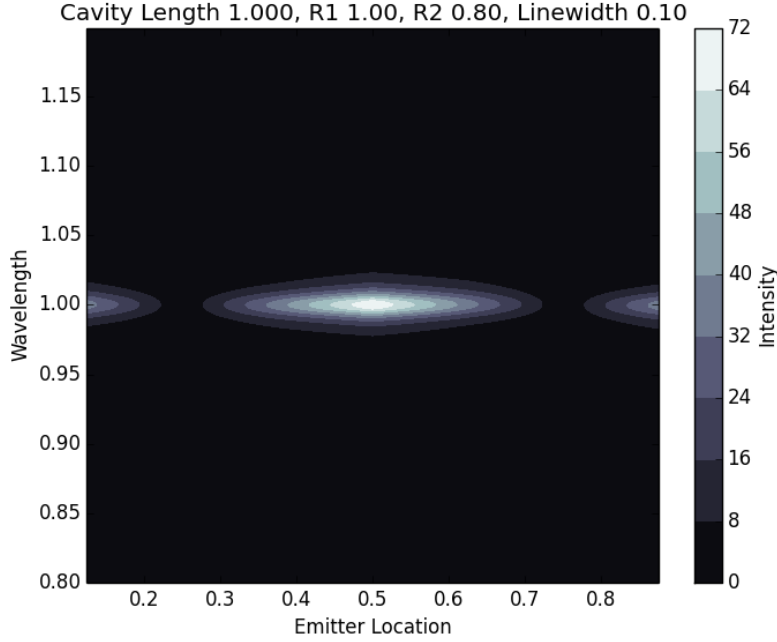


FIG. 1: Spontaneous emission output from a one wavelength cavity as a function of emitter location, with units scaled such that wavelength = 1.

reversed for stimulated emission. Classically, the suppression of spontaneous emission at the anti-nodes corresponds to destructive interference from the emitted field reflected by the mirrors. For stimulated emission, the process is driven by a photon already in the cavity mode, and the emitted photon is always in phase with the stimulating photon as well as being aligned to it.<sup>15</sup> Thus we can construct a microcavity device in which the output is nearly entirely stimulated emission by simply locating a thin emitter at the classically forbidden position for spontaneous emission.

We consider a one wavelength microcavity with  $R_1 = 1$ . Equation (2) then reduces to

$$\frac{|E_{cav}(\lambda)|^2}{|E_{free}(\lambda)|^2} = \frac{2(1 + \sqrt{R_2})}{1 - \sqrt{R_2}} \left(1 + \cos\left(4\pi \frac{x(\lambda)}{\lambda}\right)\right) \quad (3)$$

The output from spontaneous emission at the anti-node is identically zero. For a point near the anti-node  $x(\lambda) = \lambda/4 + \zeta$ , the output is

$$\frac{|E_{cav}(\lambda)|^2}{|E_{free}(\lambda)|^2} \approx \frac{1 + \sqrt{R_2}}{1 - \sqrt{R_2}} \left(4\pi \frac{\zeta}{\lambda}\right)^2 \quad (4)$$

For a thin slab centered at the anti-node we expect the contribution from spontaneous emission to fall off as the cube of the thickness.

The output from spontaneous emission at the node,  $x(\lambda) = \lambda/2$ , is

$$\frac{|E_{cav}(\lambda)|^2}{|E_{free}(\lambda)|^2} = \frac{4(1 + \sqrt{R_2})}{1 - \sqrt{R_2}} \quad (5)$$

For  $R_2$  from 10% to 90%, there is an enhancement on order of  $10^1$  to  $10^2$  for spontaneous emission into the cavity mode.

### III. MICROCAVITY DEVICES WITH STIMULATED EMISSION

Emission couples to a cavity mode as a product of the transition dipole moment and the electric field vector of the cavity mode,

$$g_k \propto \mu_{12} \cdot E_k \quad (6)$$

This means we have two ways to select for emission into a vertical cavity mode. We can construct the device with a dielectric mirror such that only vertical modes are allowed as in FIG. 2, or we can use emitters whose transition dipole moments are oriented normal to the vertical mode as in FIG. 3. These are referred to as the multi-layer mirror microcavity OLED (MLM OLED) and the symmetrized emitter microcavity OLED (SEM OLED). In both devices, the ideal configuration has a thin emitter layer located at  $x(\lambda) = (2m + 1)\lambda/4$ , and  $L(\lambda) = n\lambda/2$ , for  $m, n = 0, 1, \dots$

Emitter materials exhibiting the orientation required for the SEM OLED have been reported for vapor deposited thin films and solution deposited thin films.<sup>161718</sup> These include triplet emitters and polymers. In those reports, horizontal orientation is seen as a way to increase the vertical content of the generated light. Here we locate the emitter at a point in the microcavity where output by spontaneous emission is suppressed and instead output is dominated by stimulated emission.

We can write rate equations<sup>19</sup> for the vertical cavity mode in the proposed device architecture as

$$\frac{dN_{eh}}{dt} = \frac{\gamma I}{eV_a} - g_k P_k N_{eh} - \left( \frac{f_k}{\tau_{sp}} + \frac{1}{\tau_{nr}} + \frac{f_{RL}}{\tau_{sp}} \right) N_{eh} - \kappa N_{eh}^2 \quad (7)$$

$$\frac{dP_k}{dt} = g_k N_{eh} P_k + \frac{f_k}{\tau_{sp}} N_{eh} - \frac{P_k}{\tau_{cav}} \quad (8)$$

where  $N_{eh}$  is the density of excited state species formed by electron-hole recombination,  $\gamma$  is the charge carrier balance factor (we assume an emitter with  $\eta_{S/T} = 1$ ),  $V_a$  is the active volume,  $g_k$  is the gain coefficient for stimulated emission,  $P_k$  is the photon density,  $f_k$  is the attenuation or enhancement of spontaneous emission into the cavity mode,  $\tau_{sp}$  is the free space relaxation lifetime,  $\tau_{nr}$  is the non-radiative relaxation lifetime,  $f_{RL}$  is the coefficient for radiative loss due to spontaneous emission outside of the cavity mode,  $\kappa$  is the coefficient for second order losses including triplet-triplet annihilation,<sup>1112</sup> and  $\tau_{cav}$  is the cavity lifetime.

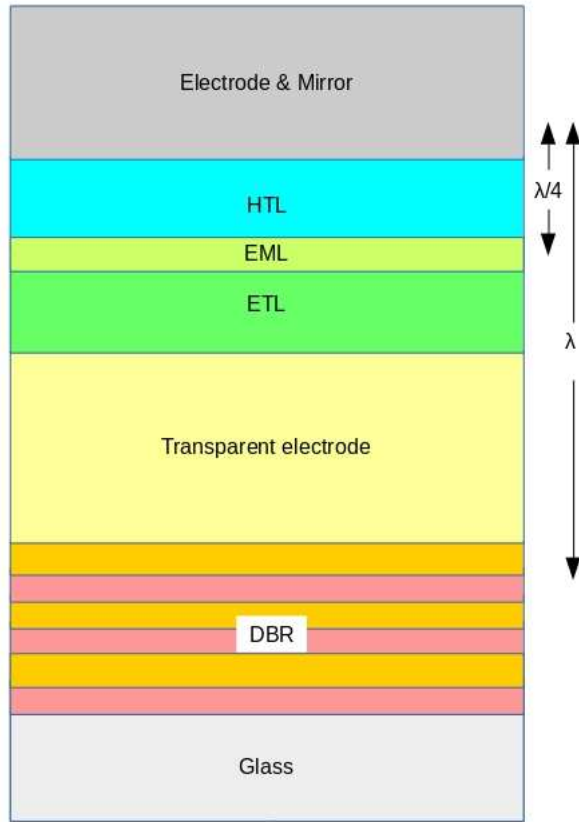


FIG. 2: MLM OLED device with Bragg reflector, optical length equal to one wavelength and emitter at the anti-node.

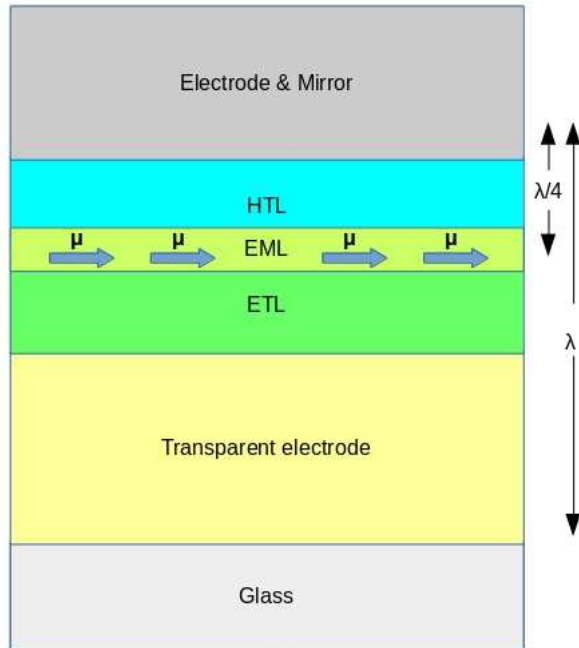


FIG. 3: SEM OLED device with emitter transition dipole moments in-plane.

The cavity lifetime, for a microcavity with optical length  $L(\lambda)$  with exit mirror reflectivity  $R$ , is given by<sup>20</sup>

$$\tau_{cav} = \frac{L(\lambda)}{2c(1 - R)} \quad (9)$$

For an optical microcavity device the cavity lifetime is on order of  $10^{-15}$  secs to  $10^{-13}$  secs for  $R \sim 1\%$  to 99%. The non-radiative and free space radiative lifetimes are on order of or greater than  $10^{-7}$  secs.

For a thin emitter located at the anti-node,  $f_k$  approaches zero, and so in steady state we obtain,

$$\frac{\gamma}{eV_a} I = \frac{P_k}{\tau_{cav}} + \left( \frac{1}{\tau_{nr}} + \frac{f_{RL}}{\tau_{sp}} \right) N_{eh} + \kappa N_{eh}^2 \quad (10)$$

and from the second rate equation,  $N_{eh}$  is a constant,

$$N_{eh} = \frac{1}{g_k \tau_{cav}} \quad (11)$$

With light output  $L$  equal to  $P_k V_a / \tau_{cav}$ , we can write equation (10) as

$$L \approx \frac{\gamma}{e} I - \Lambda \quad (12)$$

where  $\Lambda$  represents the constant loss terms.

In other words, for the microcavity device with the thin emitter at the anti-node, we expect to see linear conversion of current to light with a constant offset. As we increase current the device should become more efficient approaching an asymptote, and there should be no roll-off from quenching. With an oriented emitter the radiative losses should be smaller, and so we expect the SEM OLED with oriented emitters, to be a little more efficient at moderate output than the MLM device with randomly oriented emitters.

We consider now a microcavity with emitter at the node. Output is dominated by spontaneous emission and the steady state solution for the second rate equation gives

$$f_k \frac{N_{eh}}{\tau_{sp}} = \frac{P_k}{\tau_{cav}} \quad (13)$$

In this device the photon population is proportional to the recombined electron-hole pair population, and so the efficiency relationship becomes

$$\frac{\gamma}{eV_a} I = \frac{P}{\tau_{cav}} \left( 1 + \frac{\tau_{sp}}{f_k \tau_{nr}} + \frac{f_{RL}}{f_k} \right) + \kappa \left( \frac{\tau_{sp}}{f_k} \frac{P_k}{\tau_{cav}} \right)^2 \quad (14)$$

For comparison to the stimulated emission device, we write the efficiency relationship for the spontaneous emission device as

$$L = \left( \frac{\gamma}{e} I - \kappa' L^2 \right) \frac{f_k}{f_k + \frac{\tau_{sp}}{\tau_{nr}} + f_{RL}} \quad (15)$$

where  $\kappa' = (\kappa/V_a)(\tau_{sp}/f_k)^2$ . The efficiency relationship thus exhibits roll-off and an overall coefficient that combines enhancement, quantum efficiency and radiative losses. For a large enhancement factor  $f_k \gg f_{RL} + \tau_{sp}/\tau_{nr}$ , the overall coefficient approaches 1 (corresponding to a high finesse cavity), and the second order loss term is attenuated through the dependence of  $\kappa'$  on  $(1/f_k)^2$ . For  $f_k = 1$ , at low L, efficiency is determined by radiative versus non-radiative decay and radiative losses. Suppression with  $f_k \ll 1$  and output from spontaneous emission approaching 0, occurs only with the emitter approaching the anti-node.

Finally we consider a device with contributions from both stimulated emission and spontaneous emission. The second rate equation gives for the excited state population

$$N_{eh} = \frac{P_k/\tau_{cav}}{g_k P_k + \frac{f_k}{\tau_{sp}}} \quad (16)$$

and so  $N_{eh}$  varies with  $P_k$  similar to the spontaneous emission device over some part of its operating range. The intermediate device approaches stimulated emission ( $N_{eh}$  constant) only for  $P_k \gg f_k/g_k\tau_{sp}$ .

We note that almost any planar OLED can be described as a microcavity device (though not necessarily resonant) and will have an enhancement factor described by equation (2), and in the absence of stimulated emission, its efficiency will be as described by equation (15).

A stimulated emission device with high carrier balance and low ohmic losses, can approach unit efficiency as power is increased because the loss terms are proportional to  $N_{eh}$  which is held constant. Cavity finesse does not explicitly enter into the efficiency relationship except as the emitter layer thickness increases. A device in which spontaneous emission dominates the output might achieve unit efficiency but only if it has high carrier balance, low ohmic losses, high quantum yield, negligible radiative losses, and is operated at low power or has a very large enhancement factor. So, we expect that stimulated emission devices will generally be a more practical route to high efficiency at high power.

#### IV. EXPERIMENTAL

MLM OLED and SEM OLED devices were fabricated by thermal vapor deposition under high vacuum ( $\sim 10^{-6}$  torr).<sup>21</sup> The MLM device configuration is schematically, glass/ multilayer mirror(TiO<sub>2</sub>/ SiO<sub>2</sub>)<sub>xn</sub>/ ITO/ HTL/ EML(yellow)/ ETL/ Al/  $\sim 100\%$ DBR(TiO<sub>2</sub>/ SiO<sub>2</sub>)<sub>xn</sub>, with optical length 475 nm and emitter of optical thickness  $\sim 50$  nm centered on the first anti-node relative to the top mirror. The SEM OLED configuration is schematically glass/ ITO/ HIL/ HTL/ EBL/

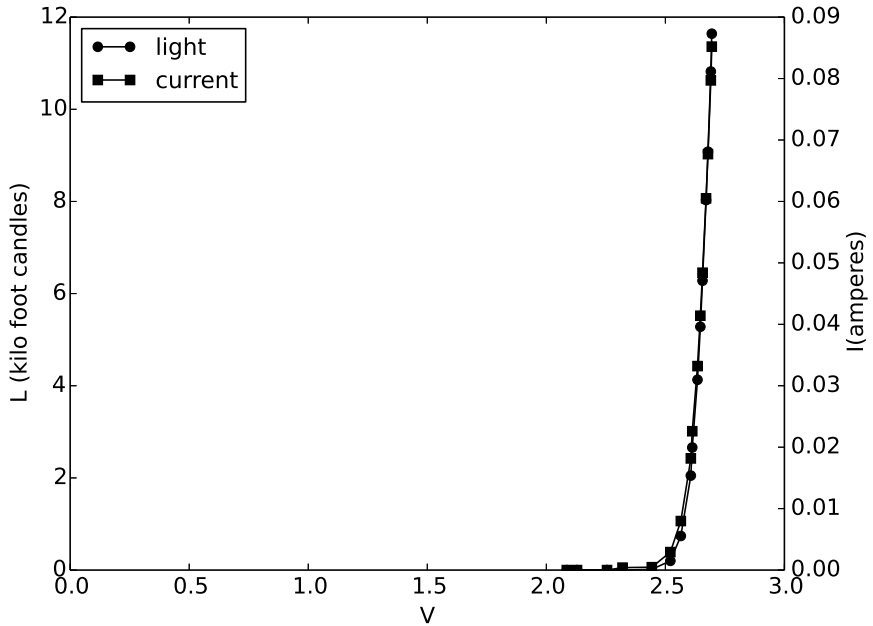


FIG. 4: L-I-V data for an MLM type OLED with emitter at quarter wavelength position.

M-CBTz:[Bt]2Ir(acac) (10%)/ ETL/ LiF (0.5nm)/ Al (10nm)/Ag (100nm), with optical length 408 nm and emitter of optical thickness 45 nm starting at the anti-node relative to the top mirror.

Light-current-voltage data for the MLM OLED is shown in FIG. 4. Power was supplied from a bench supply operated in voltage controlled mode. Current was measured across a 100 ohm resistor in series with the OLED. Bias voltage was measured across the OLED. Light was measured using an Extech EA31 with the detector at approximately 1 cm from the device. The supply voltage was incremented in 0.1 steps, and voltage setting, bias voltage, current, and light readings were recorded at each step. Power efficiency for the MLM OLED was measured independently on a separate occasion using an integrating sphere and reported as 318 lm/W.

The SEM OLED was fabricated on a pixelated anode ITO substrate (OSILLA), in a total effort of one evening for the first specimens. Luminous efficiency was measured using an ILT 1700 Research Radiometer and 10" light sphere from International Light Technologies and found to be 340 lm/W, a 10% improvement over the MLM device.

## V. DISCUSSION

As can be seen in FIG. 4, light and current take-off abruptly after about 2.6 volts. The light-current-voltage behavior is shown in more detail in FIG. 5. Light and current rise together with

current only slightly ahead of light. At 2.607 to 2.613 ( $\pm 0.006$ ) Volts, there is a small jump in current and light together, after which they quickly converge. In FIG. 6, we see that light versus current follows the expected linear relationship (equation (12)) from about 20 mA and upwards. We note that the bias voltage at the jump corresponds to a wavelength of 475 nm, which matches the cavity length, and that the transition to linear behavior occurs at this data point in FIG. 5.

In FIG. 7 we fit the current-voltage behavior to a Mott-Gurney square law with Poole-Frenkel type dependence of mobility on field,<sup>2223</sup>

$$J \propto \exp(\alpha\sqrt{V/L}) \frac{V^2}{L^3} \quad (17)$$

where carrier mobility  $\mu = \mu_0 \exp(\alpha\sqrt{V/L})$ . There are two distinct regions in the log plot with the coefficient  $\alpha$  changing from about  $71/V^{1/2}$  below the transition to about  $48/V^{1/2}$  above the transition, a factor of two on a per volt basis. The low current region can also be fit to a trap fill limit (TFL) model,<sup>24</sup>

$$J \propto V^{r+1} \quad (18)$$

where  $r = T_t/T$  and  $T_t$  is the trap energy. A log-log fit to our data in the low current region gives  $T_t \sim 1.5 \times 10^4$  K (1.2 eV). However the apparent close relationship between the change in current-voltage behavior and the transition to linear output, suggests that there may be more to learn about what is happening in charge mobility accompanying this transition.

Power efficiency for the device is graphed in FIG. 8 as kfc/W. The power efficiency increases rapidly and then appears to approach an asymptote. The end point, converted from kfc, is about 315 lm/W and is in agreement with the independent measurement of 318 lm/W. This is fairly unusual in OLEDS. It is however consistent with equation (12) for a stimulated emission device.

The SEM version of the device differs from the MLM in having a self-oriented emitter layer and omitting multi-layer mirrors. This implementation also has injection and blocking layers. However, the device in terms of optical lengths was specifically designed to implement the ideas proposed here, and at 340 lm/W it is substantially beyond the efficiency of any other device reported in the literature.

Early microcavity OLEDS show line sharpening<sup>26</sup> and enhancements in external efficiency up to a factor of four<sup>28</sup>. More recently, devices have been reported with power efficiencies at 110 lm/W and 140 lm/W.<sup>10</sup> However, those devices droop from the beginning of the reported operating range as expected from the analysis leading up to equation (15). In an extensive review of literature of microcavity OLEDS, no devices were found in which a thin emitter was located at the anti-node

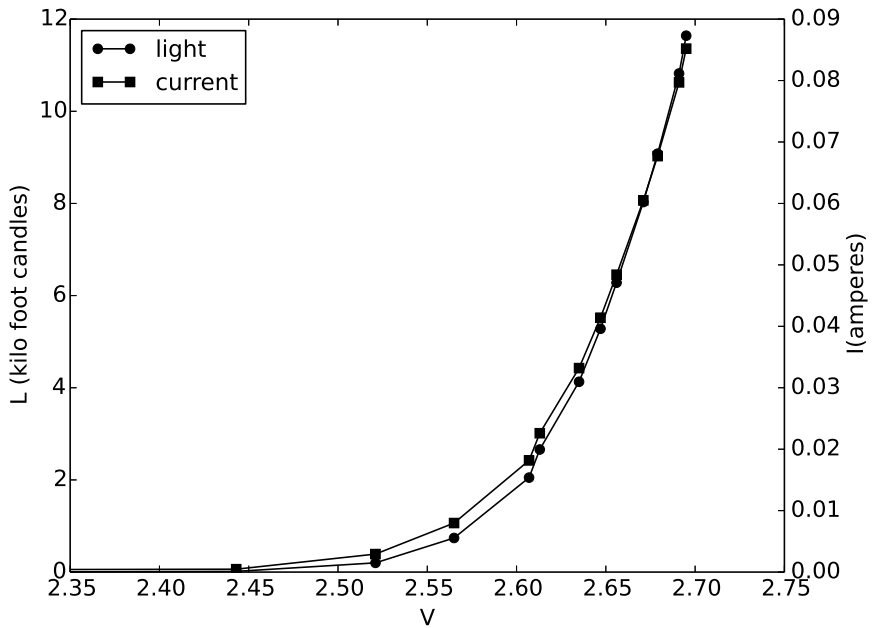


FIG. 5: Light and current versus voltage in the operating range of the device.

and no devices were found that exhibited the performance reported here. So it seems that the stimulated emission OLED is different from previous devices in terms of architecture, performance and electrical behavior.

## VI. CONCLUSIONS

The stimulated emission devices reported here, with emitter at the anti-node, demonstrate unambiguously high output well above all previously reported devices. Light versus current measured for the MLM device follows the relationship predicted in equation (12). The increasing efficiency is consistent with the linear relationship between light and current. There is possibly an interesting electrical behavior in the transition to linear output, which merits further study.

The SEM version of the device proved to be easy to make, and the first effort produced a new efficiency record for OLEDS at 340 lm/W while the MLM device achieved 315 lm/W. The analysis presented here suggests that while similar efficiency might be available in a spontaneous emission device it would be challenging to produce such a device without roll-off. The stimulated emission OLED therefore seems to offer some advantages over spontaneous emission devices, and the SEM

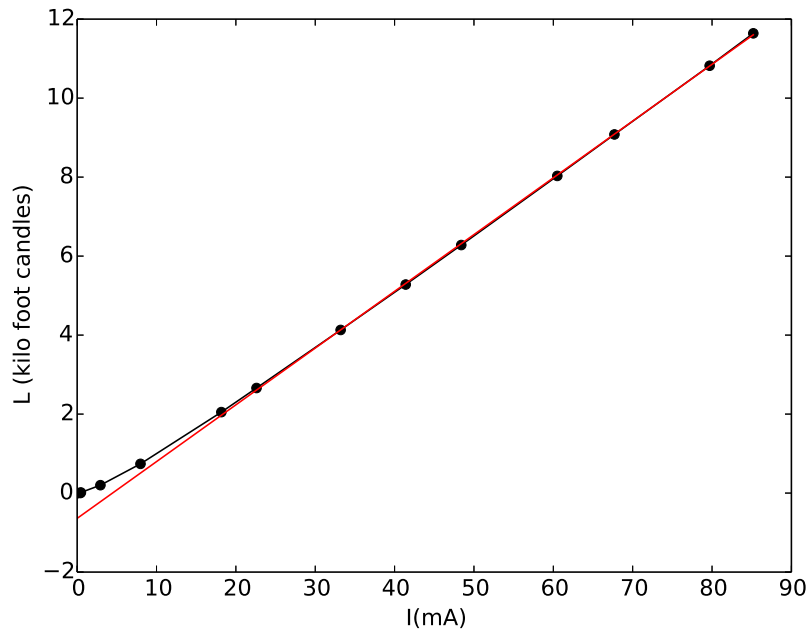


FIG. 6: Light versus current. The behavior is linear from 20 mA, with a small negative offset.

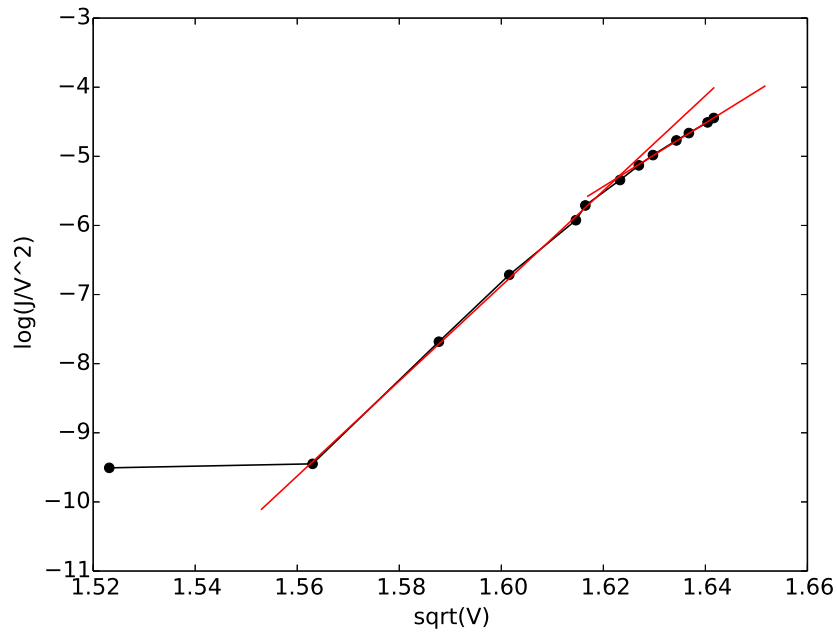


FIG. 7: Log mobility square root of voltage for the MLM. The change in slope occurs at the transition to linear light versus current.

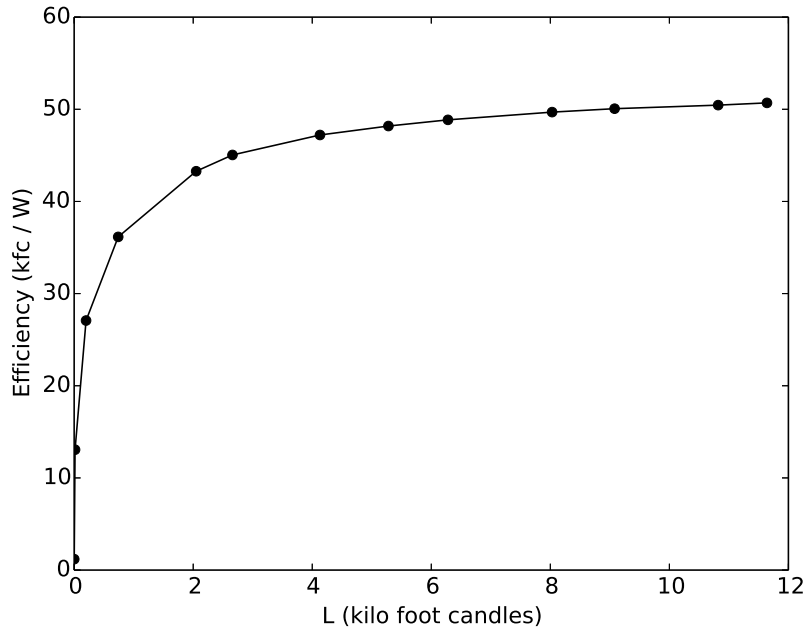


FIG. 8: Power efficiency as kfc/W. The efficiency curve increases and appears to approach an asymptote.

OLED in particular may be a useful and relatively easy to make, high efficiency OLED.

---

<sup>1</sup> Light's Labour's Lost Policies for Energy efficient Lighting, In support of the G8 Plan of Action, International Energy Agency, 2006, <http://www.iea.org/textbase/npsum/lll.pdf>

<sup>2</sup> N. L. Lam, Y. Chen, C. Weyant, C. Venkataraman, P. Sadavarte, M. A. Johnson, K. R. Smith, B. T. Brem, J. Arineitwe, J. E. Ellis, and T. C. Bond, *Environ. Sci. Technol.* 46 (24), pp 1353113538 (2012)

<sup>3</sup> R. Provoost and M. Goetzeler, A Global transition to efficient lighting, United Nations Environmental Programme (UNEP) 2012

<sup>4</sup> M. Pope, H. P. Kallmann, and P. Magnante, *J. Chem. Phys.* 38, 2042 (1963)

<sup>5</sup> C. W. Tang and S. A. VanSlyke, *Appl. Phys. Lett.* 51, 913 (1987)

<sup>6</sup> C. Adachi, T. Tsutsui, and S. Saito, *Appl. Phys. Lett.* 57, 531 (1990)

<sup>7</sup> R. Sebastian, M. Thomschke, B. Lssem, K. Leo., *Rev. Mod. Phys.* 85(3), 1245-1293 (2013)

<sup>8</sup> T. Tsutsui and N. Takada, *Jpn. J. Appl. Phys.* 52 110001 (2013)

<sup>9</sup> W. Brütting, J. Frischeisen, T. D. Schmidt, B. J. Scholz, and C. Mayr, C., *Phys. Status Solidi A* 210, 4465 (2013)

<sup>10</sup> S. Reineke, F. Lindner, G. Schwartz, N. Seidler, K. Walzer, B. Lussem, and L. Leo, *Nature* 459, 234-238 (2009)

<sup>11</sup> M. A. Baldo, C. Adachi, and S. R. Forrest, *Phys. Rev. B* 62, 10967 (2000)

<sup>12</sup> S. Reineke, K. Walzer, and K. Leo, Phys. Rev. B 75, 125328 (2007)

<sup>13</sup> D. G. Deppe, C. Lei, C. C. Lin, and D. L. Huffaker, J. Mod. Opt. 41(2), 325-344 (1994)

<sup>14</sup> A. Dodabalapur, L. J. Rothberg, R. H. Jordan, T. M. Miller, R. E. Slusher, and J. M. Phillips, J. Appl. Phys. 80(12) 6954-6964 (1996)

<sup>15</sup> A. Einstein, Physikalische Zeitschrift 18, 121 (1917)

<sup>16</sup> S. Kim, W. Jeong, C. Mayr, Y. Park, K. Kim, J. Lee, C. Moon, W. Brutting, and J. Kim, Adv. Func. Mater. 23, 3896-3900 (2013)

<sup>17</sup> N. C. Greenham, R. H. Friend, and D. D. C. Bradley, Adv. Mater. 6(6) 491-494 (1994)

<sup>18</sup> T. D. Schmidt, D. S. Setz, M. Flammich, J. Frischeisen, D. Michaelis, C. Mayr, A. F. Rausch, T. Welhus, B. J. Scholz, T. C. G. Reusch, N. Danz, and W. Brutting, Appl. Phys. Lett. 103, 093303 (2013)

<sup>19</sup> G. P. Agrawal and N. K. Dutta, *Semiconductor Lasers*, Second Edition, (VanNostrand Reinhold, New York, 1993), chapter 6

<sup>20</sup> M. Fox, *Quantum Optics*, (Oxford University Press, 2014), chapter 10

<sup>21</sup> Fabricated by J. Magno, R. B. Wison and G. Koch.

<sup>22</sup> A. Ioannidis, E. Forsythe, Y. Gao, M. W. Wu, E. M. Conwell, Appl. Phys. Lett. 72(23), 3038 (1998)

<sup>23</sup> H. Bassler and A. Kohler, Top. Curr. Chem. 312, 1-66 (2012)

<sup>24</sup> P. W. M. Blom and M. C. J. M. Vissenberg, Mat. Sci. Eng. 29, 53-94 (2000)

<sup>25</sup> O. Kwon, B. D. Kim, W. Kim, B. Lee, and Y. Kwon, Nanotechnology Materials and Devices Conference, Vol 1, 366-367 (2006)

<sup>26</sup> N. Takada, T. Tsutsui, and S. Saito, Appl. Phys. Lett. 63(15) 2032-2034 (1993)

<sup>27</sup> A. Carbone, B. K. Kotowoska, D. Kotowoski, Phys. Rev. Lett. 95, 236601 (2005)

<sup>28</sup> R. Jordan, A. Dodabalapur, and R. E. Slusher, Appl. Phys. Lett. 69, 1997 (1996)

<sup>29</sup> L. R. Brovelli, and U. Keller, Opt Comm. 116, 343-350 (1995)

<sup>30</sup> C. J. R. Sheppard, Pure ppl. Opt. 4, 665-669 (1995)